Inorg. Chem. **1991**, *30*, 4909–4914

Contribution from the Department of Chemistry, University of Wyoming, Laramie, Wyoming 82071,
and Chemistry Laboratory I. H. C. Ørsted Institute, Universitetsparken 5, DK-2100 Copenhagen Ø, Denmark

Syntheses and Characterization of Binuclear Manganese(III,IV) and -(IV,IV) Complexes with Ligands Related to *N*,*N*′-Bis(2-pyridylmethyl)-1,2-ethanediamine

Patricia A. Goodson,[1a] Jørgen Glerup,[1b] Derek J. Hodgson,*[,1a] Kirsten Michelsen,*[,1b] and Høgni Weihe[1b]

Received April 30, 1991

The synthesis and characterization of several new bis(μ-oxo)dimanganese(III,IV) and -(IV,IV) complexes employing tetradentate ligands related to *N*,*N*′-bis(2-pyridylmethyl)-1,2-ethanediamine (bispicen) (**1**) are reported. The crystal structure of one Mn^{IV}_2 complex, bis(μ-oxo)bis[*N*,*N*′-bis(2-pyridylmethyl)-1,3-propanediamine]dimanganese(IV,IV) perchlorate trihydrate, [(bispictn)-Mn–O_2–Mn(bispictn)]$(ClO_4)_4 \cdot 3H_2O$ (**14**), has been established by three-dimensional X-ray diffraction techniques. The complex, of formula $Mn_2C_{30}H_{44}N_8O_{20}Cl_4$, crystallizes in the monoclinic space group $P2_1/c$ with four molecules in a cell of dimensions a = 12.772 (7) Å, b = 18.581 (7) Å, c = 18.816 (6) Å, and β = 108.81 (3)°. The structure was solved by direct methods and refined by least-squares techniques to a final agreement factor of 0.0564 based on 2247 observed independent intensities. The structure is similar to that of the bispicen analogue, but the Mn–Mn distance of 2.719 (3) Å is longer than that of 2.672 (1) Å in the bispicen complex, and the bridging Mn–O–Mn angles of 98.4 (4) and 97.3 (4)° are larger than those of 95.0 (2) and 95.2 (2)° in the bispicen complex. The magnetic properties of the (III,IV) complexes are consistent with a doublet ground state, the observed J values being similar to those observed in other (III,IV) complexes. The (IV,IV) complexes have singlet ground states, with J values again consistent with those in other systems. The EPR spectra of the (III,IV) complexes exhibit the commonly occurring 16-line spectrum, with varying degrees of anisotropy depending on the particular ligand system. The complexes all exhibit two *quasi*-reversible waves in the cyclic voltammograms, with redox potentials in the range 0.083–0.170 and 0.943–1.008 V (vs Ag/AgCl) for the (III,III) $\leftrightarrow$ (III,IV) and (III,IV) $\leftrightarrow$ (IV,IV) couples, respectively.

Introduction

The synthesis and chemical and physical properties of bridged binuclear manganese complexes have received significant recent attention, largely as a result of the importance of high-oxidation-state manganese species in biological systems but also because of their potential use as redox catalysts. Following the successful isolation of the 2,2′-bipyridine (bpy)[2] and 1,10-phenanthroline (phen)[3] complexes of the types $[L_2MnO]_2^{3+,4+}$, we[4-10] and others[11-15] have recently examined a number of bis(μ-oxo)dimanganese dimers using tetradentate ligands in place of the bidentate bpy and phen in the hope of reducing the labilities of the various binuclear species which are involved in the (IV,IV) $\leftrightarrow$ (III,IV) and (III,IV) $\leftrightarrow$ (III,III) couples. In addition to the more common $Mn^{III}Mn^{IV}$ systems, we[6,10] have reported the isolation of several Mn(III,III) species, and we and others have characterized Mn^{IV}_2 complexes.[3,7,9,15-17] In our recent report on the bis(μ-oxo)dimanganese system with the ligand *N*,*N*′-bis(2-pyridylmethyl)-1,2-ethanediamine (bispicen) (**1**),[7] we examined the redox potentials of this complex in an attempt to analyze its ability to serve as an electroactive redox catalyst. Since a primary goal of our research is to obtain a variety of complexes with a diverse range of redox potentials, we have attempted to chemically modify the ligands so as to bring about stereochemical and/or electronic changes at the metal centers. We have, therefore, undertaken a comprehensive study on a series of tetradentate ligands derived from bispicen, and report the syntheses, structural, and spectroscopic characterization of these new complexes. The ligands employed are *N*,*N*′-bis(2-pyridylmethyl)-1,3-propanediamine (bispictn) (**2**), *N*,*N*′-bis(2-pyridylmethyl)-1,2-propanediamine (bispicpn) (**3**), *N*,*N*′-bis(2-pyridylmethyl)-2,3-butanediamine (bispicbn) (**4**), *N*,*N*′-bis(2-pyridylmethyl)-1,2-cyclohexanediamine (bispichxn) (**5**), *N*,*N*′-bis(1-(2-pyridyl)ethyl)-1,2-ethanediamine (Me_2bispicen) (**6**), and *N*,*N*′-bis(1-(2-pyridyl)ethyl)-1,3-propanediamine (Me_2bispictn) (**7**).

Experimental Section

Syntheses. The ligands were synthesized by modifications of previously reported methods for the synthesis of bispicen (**1**).[18,19] The syntheses of bispictn (**2**), and bispicpn (**3**) have been reported elsewhere.[20,21] The ligands **4** and **5** were prepared in an analogous method using the appropriate diamine and pyridine-2-carboxaldehyde. The amines used were $(-)_D$-1,2-propanediamine (for **3**), racemic 2,3-butanediamine (for **4**), and $(-)_D$-1,2-cyclohexanediamine (for **5**). Ligands **6** and **7** were prepared from 2-acetylpyridine and the appropriate diamine, 1,2-ethanediamine (for **6**) and 1,3-propanediamine (for **7**).

Bis(μ-oxo)bis[*N*,*N*′-bis(2-pyridylmethyl)-1,3-propanediamine]dimanganese(III,IV) Perchlorate Trihydrate, [(bispictn)Mn–O_2–Mn(bispictn)]$(ClO_4)_3 \cdot 3H_2O$ (8). Bispictn·4HCl·2H_2O (424 mg, 1 mmol) was dissolved in water (2 mL). A solution of sodium carbonate (2.5 mL, 1 M) was added, followed by $MnCl_2 \cdot 4H_2O$ (197 mg, 1 mmol). A solution of hydrogen peroxide (1.5 mL, 1 M) was added dropwise with stirring. The solution immediately changed color to green-black. After being stirred for 15 min, the solution was filtered. The filtrate was cooled on ice, and a solution of sodium perchlorate (1 g in 1–2 mL) was added slowly with stirring to separate out olive green crystals. The crystals were collected by filtration and washed with a solution of sodium perchlorate (1 M) and with a mixture of ethanol and ether (60/40). The yield of practically pure complex was 392 mg (77%). The crude product was recrystallized from boiling water to give 258 mg (51%) of large black-green crystals. Anal. Calcd for $Mn_2C_{30}H_{46}Cl_3N_8O_{17}$: Mn, 10.91; C,

---

(1) (a) University of Wyoming. (b) H. C. Ørsted Institute.

(2) (a) Nyholm, R. S.; Turco, A. *Chem. Ind.* (*London*) **1960**, 74. (b) Plaksin, P. M.; Stoufer, R. C.; Mathew, M.; Palenik, G. J. *J. Am. Chem. Soc.* **1972**, *94*, 2121–2122.

(3) (a) Goodwin, H. A.; Sylva, R. N. *Aust. J. Chem.* **1967**, *20*, 629–637. (b) Stebler, M.; Ludi, A.; Bürgi, H.-B. *Inorg. Chem.* **1986**, *25*, 4743–4750.

(4) Collins, M. A.; Hodgson, D. J.; Michelsen, K.; Pedersen, E. *J. Chem. Soc., Chem. Commun.* **1987**, 1659–1660.

(5) Towle, D. K.; Botsford, C. A.; Hodgson, D. J. *Inorg. Chim. Acta* **1988**, *141*, 167–168.

(6) Goodson, P. A.; Hodgson, D. J. *Inorg. Chem.* **1989**, *28*, 3606–3608.

(7) Goodson P. A.; Glerup, J.; Hodgson, D. J.; Michelsen, K.; Pedersen, E. *Inorg. Chem.* **1990**, *29*, 503–508.

(8) Goodson, P. A.; Hodgson, D. J.; Michelsen, K. *Inorg. Chim. Acta* **1990**, *172*, 49–57.

(9) Oki, A. R.; Glerup, J.; Hodgson, D. J. *Inorg. Chem.* **1990**, *29*, 2435–2441.

(10) Goodson, P. A.; Oki, A. R.; Glerup, J.; Hodgson, D. J. *J. Am. Chem. Soc.* **1990**, *112*, 6248–6254.

(11) Hagen, K. S.; Armstrong, W. H.; Hope, H. *Inorg. Chem.* **1988**, *141*, 167–168.

(12) Brewer, K. J.; Liegeois, A.; Otvos, J. W.; Calvin, M.; Spreer, L. O. *J. Chem. Soc., Chem. Commun.* **1988**, 1219–1220.

(13) Suzuki, M.; Senda, H.; Kobayashi, Y.; Oshio, H.; Uehara, A. *Chem. Lett.* **1988**, 1763–1766.

(14) Spreer, L. O. Private communication. Brewer, K. J.; Calvin, M.; Lumpkin, R. S.; Otvos, J. W.; Spreer, L. O. *Inorg. Chem.* **1989**, *28*, 4446–4451.

(15) Suzuki, M.; Tokura, S.; Suhara, M.; Uehara, A. *Chem. Lett.* **1988**, 477–480.

(16) Wieghardt, K.; Bossek, U.; Nuber, B.; Weiss, J.; Bonvoisin, J.; Corbella, M.; Vitols, S. E.; Girerd, J. J. *J. Am. Chem. Soc.* **1988**, *110*, 7398–7411.

(17) Libby, E.; Webb, R. J.; Streib, W. E.; Folting, K.; Huffman, J. C.; Hendrickson, D. N.; Christou, G. *Inorg. Chem.* **1989**, *28*, 4037–4040.

(18) Goodwin, H. A.; Lions, F. *J. Am. Chem. Soc.* **1960**, *82*, 5013–5023.

(19) Heinrichs, M. A.; Hodgson, D. J.; Michelsen, K.; Pedersen, E. *Inorg. Chem.* **1984**, *23*, 3174–3180.

(20) Fischer, H. R.; Hodgson, D. J.; Michelsen, K.; Pedersen, E. *Inorg. Chim. Acta* **1984**, *88*, 143–150.

(21) Michelsen, K.; Nielsen, K. M. *Acta Chem. Scand., Ser. A* **1980**, *A34*, 755–764.

0020-1669/91/1330-4909$02.50/0 © 1991 American Chemical Society

35.78; H, 4.60; Cl, 10.56, N, 11.13. Found: Mn, 10.90; C, 36.05; H, 4.12; Cl, 10.42; N, 11.08.

Bis(μ-oxo)bis[*N*,*N*′-bis(2-pyridylmethyl)-1,2-propanediamine]dimanganese(III,IV) Perchlorate Pentahydrate, [(bispicpn)Mn–O_2–Mn(bispicpn)]$(ClO_4)_3 \cdot 5H_2O$ (9). The complex was synthesized from bispicpn·$4HCl \cdot 2H_2O$ (438 mg, 1 mmol) following the same procedure as described for **8** above. The yield of pure material was 219 mg (42%). Anal. Calcd for $Mn_2C_{30}H_{50}Cl_3N_8O_{19}$: Mn, 10.54; C, 34.55; H, 4.63; Cl, 10.20; N, 10.74. Found: Mn, 10.49; C, 34.46; H, 4.21; Cl, 10.18; N, 10.71.

Bis(μ-oxo)bis[*N*,*N*′-bis(2-pyridylmethyl)-2,3-butanediamine]dimanganese(III,IV) Perchlorate Tetrahydrate, [(bispicbn)Mn–O_2–Mn(bispicbn)]$(ClO_4)_3 \cdot 4H_2O$ (10). The complex was synthesized from bispicbn·$4HCl \cdot 3.5H_2O$ (479 mg, 1 mmol) following the same procedure as described for **8** above. The sticky crude product was recrystallized from boiling water to give 141 mg (27%) of pure product. Anal. Calcd for $Mn_2C_{32}H_{52}Cl_3N_8O_{18}$: Mn, 10.43; C, 36.50; H, 4.98; Cl, 10.10; N, 10.64. Found: Mn, 10.36; C, 36.67; H, 4.48; Cl, 10.06; N, 10.67.

Bis(μ-oxo)bis[*N*,*N*′-bis(2-pyridylmethyl)-1,2-cyclohexanediamine]dimanganese(III,IV) Perchlorate Pentahydrate, [(bispichxn)Mn–O_2–Mn(bispichxn)]$(ClO_4)_3 \cdot 5H_2O$ (11). The complex was synthesized from bispichxn·$4HCl \cdot 2H_2O$ (485 mg, 1 mmol) following the same procedure as described for **8** above. The crude product was recrystallized from boiling water to give 346 mg (62%) of pure product. Anal. Calcd for $Mn_2C_{36}H_{58}Cl_3N_8O_{19}$: Mn, 9.79; C, 38.48; H, 5.21; Cl, 9.47; N, 9.98. Found: Mn, 9.73; C, 38.50; H, 4.86; Cl, 9.60; N, 9.95.

Bis(μ-oxo)bis[*N*,*N*′-bis(1-(2-pyridyl)ethyl)-1,2-ethanediamine]dimanganese(III,IV) Perchlorate Monohydrate, [(Me_2bispicen)Mn–O_2–Mn(Me_2bispicen)]$(ClO_4)_3 \cdot H_2O$ (12). Me_2bispicen (245 mg, 0.920 mmol) was dissolved in water (6 mL) and $Mn(ClO_4)_2 \cdot 6H_2O$ (333 mg, 0.920 mmol) was added. The solution slowly turned dark green without any added external oxidant. After 2 days, the liquid was decanted from a gummy material, and after 1 week the solution was filtered to give 64 mg of a dark green powder. Over a period of 11 days more complex precipitated to give a combined yield of 125 mg (27%). Anal. Calcd for $Mn_2C_{32}H_{46}Cl_3N_8O_{15}$: C, 38.47; H, 4.64; Cl, 10.65; N, 11.22. Found: C, 38.38; H, 4.53; Cl, 10.57; N, 11.22.

Bis(μ-oxo)bis[*N*,*N*′-bis(1-(2-pyridyl)ethyl)-1,3-propanediamine]dimanganese(III,IV) Perchlorate, [(Me_2bispictn)Mn–O_2–Mn(Me_2bispictn)]$(ClO_4)_3$ (13). Me_2bispictn (489 mg, 1.72 mmol) was dissolved in water (5 mL), and $Mn(ClO_4)_2 \cdot 6H_2O$ (622 mg, 1.72 mmol) was added. The solution turned a darker yellow and a light precipitate formed. About 150 mg of 30% hydrogen peroxide was added dropwise. The mixture was filtered, and 225 mg (25%) of a dark green solid was collected from the filtrate after 9 days. Anal. Calcd for $Mn_2C_{34}H_{48}Cl_3N_8O_{14}$: C, 40.47; H, 4.79; Cl, 10.54; N, 11.10. Found: C, 40.51; H, 4.74; Cl, 10.26; N, 11.10.

Bis(μ-oxo)bis[*N*,*N*′-bis(2-pyridylmethyl)-1,3-propanediamine]dimanganese(IV,IV) Perchlorate Trihydrate, [(bispictn)Mn–O_2–Mn(bispictn)]$(ClO_4)_4 \cdot 3H_2O$ (14). This complex was prepared by the disproportionation of the (III,IV) dimer in perchloric acid solution in a manner analogous to that we reported for the bispicen analogue.[7] The yield was 15%. Anal. Calcd for $Mn_2C_{30}H_{46}Cl_4N_8O_{21}$: Mn, 9.94; C, 32.59; H, 4.19; Cl, 12.77; N, 10.13. Found: Mn, 9.95; C, 32.79; H, 4.08; Cl, 12.95; N, 10.09.

Bis(μ-oxo)bis[*N*,*N*′-bis(2-pyridylmethyl)-2,3-butanediamine]dimanganese(IV,IV) Perchlorate Trihydrate, [(bispicbn)Mn–O_2–Mn(bispicbn)]$(ClO_4)_4 \cdot 3H_2O$ (15). This complex was prepared by the disproportionation of the (III,IV) dimer in perchloric acid solution in a manner analogous to that reported for the bispictn complex above. The yield was 27%. Anal. Calcd for $Mn_2C_{32}H_{50}Cl_4N_8O_{21}$: Mn, 9.69; C, 33.90; H, 4.44; Cl, 12.45; N, 9.88. Found: Mn, 9.47; C, 33.65; H, 4.19; Cl, 12.42; N, 9.85.

Bis(μ-oxo)bis[*N*,*N*′-bis(2-pyridylmethyl)-1,2-cyclohexanediamine]dimanganese(IV,IV) Perchlorate Tetrahydrate, [(bispichxn)Mn–O_2–Mn(bispichxn)]$(ClO_4)_4 \cdot 4H_2O$ (16). This complex was prepared by the disproportionation of the (III,IV) dimer in perchloric acid solution in a manner analogous to that reported for the bispictn complex above. The yield was 24%. Anal. Calcd for $Mn_2C_{36}H_{56}Cl_4N_8O_{22}$: Mn, 9.13; C, 35.90; H, 4.69; Cl, 11.73; N, 9.31. Found: Mn, 8.93; C, 35.76; H, 4.69; Cl, 11.98; N, 9.39.

Spectroscopy. Electronic absorption spectra were recorded on a Hitachi SPEC 100-80 or on a Varian/Cary 2390 spectrometer in acetonitrile as solvent. EPR spectra were recorded at liquid-helium temperature on a Bruker ESP 300 spectrometer operating at a frequency of 9.38 GHz (X-band) with magnetic field modulation of 100 kHz, modulation amplitude of 7 G, and microwave power of 10 mW. Samples were examined as frozen glasses in *N*-methylformamide solution. Circular dichroism spectra were recorded on a Roussel-Jouan Dicrograhe I spectrometer.

Table I. Crystallographic and Data Collection Parameters for **14**

formula: $Mn_2C_{30}H_{44}N_8O_{20}Cl_4$
color: orange-yellow
syst: monoclinic
space group: $P2_1/c$
cell dimens:
$a = 12.772\ (7)$ Å
$b = 18.581\ (7)$ Å
$c = 18.816\ (6)$ Å
$\beta = 108.81\ (3)°$
volume = 4227 (3) Å^3
$Z = 4$

$F(000) = 2224$
$T = 23.0$ °C
abs coeff: 0.92 mm^{-1}
index ranges:
$0 \le h \le 12$
$0 \le k \le 18$
$-18 \le l \le 17$
no. of reflections: 4556
no. of obsd indep reflcns: 2247 [$I \ge 3\sigma(I)$]
$R = 0.0564$
$R_w = 0.0599$

Magnetochemistry. Magnetic susceptibilities of powdered samples were measured by the Faraday method in the temperature range 4–300 K at a field strength of 1.3 T. The magnetic field was calibrated with $Hg[Co(NCS)_4]$.[22] A detailed description of the instrumentation has been published elsewhere.[23,24] The molar susceptibilities were corrected for ligand diamagnetism using Pascal's constants.

Electrochemistry. Cyclic voltammetry was performed on a BAS-100A electrochemical analyzer using a platinum working electrode. Voltages are reported relative to Ag/AgCl. Solutions were 2×10^{-3} M in manganese complex in acetonitrile with 0.1 M tetraethylammonium perchlorate as supporting electrolyte.

X-ray Crystallography. Bis(μ-oxo)bis[*N*,*N*′-bis(2-pyridylmethyl)-1,3-propanediamine]dimanganese(IV,IV) Perchlorate Trihydrate, [(bispictn)Mn–O_2–Mn(bispictn)]$(ClO_4)_4 \cdot 3H_2O$ (14). The crystal structure of the perchlorate salt of the Mn^{IV}_2 complex was determined at 23 °C on a Nicolet R3m/V diffractometer equipped with a molybdenum tube ($\lambda(K\alpha_1) = 0.70926$ Å; $\lambda(K\alpha_2) = 0.71354$ Å) and a graphite monochromator. Experimental details and cell constants are collected in Table I. The structure was solved by direct and difference Fourier methods and refined by full-matrix least-squares techniques. The programs used were from the SHELXTL system.[25] Hydrogen atoms were placed in calculated positions (C–H = 0.96 Å), while other non-carbon atoms were refined anisotropically; because of the large number of variables in the structure, carbon atoms were refined isotropically. Final values of the agreement factors are $R = 0.0564$ and $R_w = 0.0599$ based on 2247 independent intensities with $I \ge 3\sigma(I)$. The positional parameters of the non-hydrogen atoms are presented in Table II. Hydrogen atom coordinates, anisotropic librational parameters, and observed and calculated structure amplitudes are available as supplementary material.

Results and Discussion

The $Mn^{III}Mn^{IV}$ Complexes. Electrochemistry. The cyclic voltammograms of the (III,IV) complexes all show two *quasi*-reversible redox couples, the lower potential wave corresponding to the one-electron process $Mn^{III}Mn^{IV} \leftrightarrow Mn^{III}_2$ while the higher potential wave corresponds to the $Mn^{III}Mn^{IV} \leftrightarrow Mn^{IV}_2$ couple. The electrochemical data for these processes are listed in Table III. In each case, only small changes are observed in the redox potentials when compared to the "parent" bispicen complex, which exhibits redox couples at 0.125 and 0.959 V (vs Ag/AgCl). For the $Mn^{III}Mn^{IV} \leftrightarrow Mn^{III}_2$ couple the largest change is an increase by 45 mV, while for the $Mn^{III}Mn^{IV} \leftrightarrow Mn^{IV}_2$ couple we see at most only an increase by 49 mV. It is intriguing that methylation on the carbon center α to the pyridine ring causes a decrease in the redox potentials compared to the "parent" bispicen complex, yet the same substitution causes an increase in the redox potentials in the bispictn system.

It is probable that this apparent aberration is due to steric changes at the metal center rather than to electronic factors. In general, such minor alkylation on the bispicen framework and chelate ring expansion displayed in these complexes does not appear to sterically or electronically affect the electrochemistry of the system significantly. This is in marked contrast to our recent work, where we have illustrated that appropriate modification of the pyridyl moiety, both sterically and electronically, can lead to dramatic increases in the redox potentials and isolation of the

---

(22) Figgis, B. N.; Nyholm, R. S. *J. Chem. Soc.* **1958**, 4190.
(23) Josephsen, J.; Pedersen, E. *Inorg. Chem.* **1977**, *16*, 2534–2538.
(24) Pedersen, E. *Acta Chem. Scand.* **1972**, *26*, 333–342.
(25) Sheldrick, G. M. *SHELXTL-PLUS Crystallographic System, Version 2*; Nicolet XRD Corp.: Madison, WI, 1987.

Table II. Atomic Coordinates ($\times 10^4$) and Equivalent Isotropic Displacement Parameters ($Å^2 \times 10^3$)

	x	*y*	*z*	*U*(eq),[a] $Å^2$
Mn(1)	7221 (2)	1917 (1)	5594 (1)	17 (1)
Mn(2)	7294 (2)	3283 (1)	6125 (1)	17 (1)
O(1)	7141 (7)	2821 (4)	5255 (4)	22 (4)
O(2)	7342 (7)	2377 (4)	6472 (4)	21 (3)
N(1A)	8837 (8)	1824 (5)	5761 (6)	22 (4)
N(2A)	7547 (9)	940 (5)	6115 (6)	31 (5)
N(1B)	5599 (8)	1762 (5)	5378 (5)	18 (4)
N(2B)	6792 (8)	1581 (5)	4487 (6)	23 (4)
N(1C)	8938 (9)	3371 (6)	6525 (6)	25 (4)
N(2C)	7473 (9)	4212 (5)	5583 (6)	23 (4)
N(1D)	5644 (8)	3405 (5)	5886 (6)	19 (4)
N(2D)	7192 (8)	3742 (5)	7093 (5)	22 (4)
C(2A)	9378 (11)	2189 (7)	5367 (7)	26 (4)
C(3A)	10494 (12)	2103 (7)	5497 (8)	38 (4)
C(4A)	11029 (13)	1629 (7)	6058 (8)	46 (4)
C(5A)	10492 (13)	1269 (8)	6449 (8)	39 (4)
C(6A)	9384 (12)	1354 (7)	6285 (8)	29 (4)
C(7A)	8669 (11)	1009 (7)	6677 (7)	30 (4)
C(8A)	7517 (12)	266 (8)	5613 (8)	39 (4)
C(9A)	6713 (15)	287 (9)	4856 (9)	27 (5)
C(9B)	7695 (46)	323 (28)	5005 (28)	27 (5)
C(2B)	5078 (10)	1707 (6)	5892 (7)	21 (3)
C(3B)	3941 (11)	1626 (7)	5696 (7)	30 (4)
C(4B)	3329 (12)	1592 (7)	4952 (7)	33 (4)
C(5B)	3858 (11)	1653 (7)	4408 (8)	29 (4)
C(6B)	4988 (11)	1728 (7)	4637 (7)	22 (3)
C(7B)	5648 (10)	1820 (7)	4127 (7)	27 (4)
C(8B)	6988 (12)	809 (7)	4336 (8)	36 (4)
C(2C)	9577 (11)	2969 (7)	7096 (7)	25 (3)
C(3C)	10732 (12)	3045 (8)	7349 (8)	39 (4)
C(4C)	11184 (13)	3551 (7)	7003 (8)	43 (4)
C(5C)	10521 (12)	3972 (7)	6420 (8)	38 (4)
C(6C)	9384 (11)	3855 (7)	6172 (7)	26 (4)
C(7C)	8558 (11)	4229 (7)	5508 (8)	33 (4)
C(8C)	7162 (11)	4930 (7)	5885 (7)	29 (4)
C(9CD)	7677 (11)	4985 (7)	6719 (7)	29 (4)
C(2D)	4910 (10)	3413 (6)	5172 (7)	21 (3)
C(3D)	3794 (11)	3442 (7)	5071 (7)	27 (3)
C(4D)	3403 (12)	3457 (7)	5684 (7)	34 (4)
C(5D)	4205 (12)	3453 (7)	6405 (8)	36 (4)
C(6D)	5284 (11)	3417 (7)	6486 (7)	23 (3)
C(7D)	6188 (10)	3389 (7)	7208 (7)	26 (4)
C(8D)	7065 (11)	4557 (6)	7151 (7)	29 (4)
Cl(1)	−222 (3)	8667 (2)	1115 (2)	41 (2)
O(3)	516 (11)	8138 (7)	1583 (11)	56 (7)
O(4)	−110 (17)	9326 (9)	1507 (11)	101 (11)
O(5)	−1290 (16)	8400 (14)	1096 (17)	153 (15)
O(6)	−238 (29)	8706 (13)	419 (10)	168 (18)
O(3A)	−1167 (44)	8653 (27)	515 (32)	40 (17)
O(4A)	−583 (57)	8818 (38)	1630 (33)	69 (22)
O(5A)	416 (50)	8084 (32)	1021 (42)	70 (22)
O(6A)	697 (60)	9184 (37)	1093 (39)	107 (29)
Cl(2)	5991 (17)	−70 (12)	7152 (13)	32 (7)
O(7)	5091 (21)	−90 (16)	7302 (19)	65 (12)
O(8)	6304 (17)	−805 (11)	7124 (10)	60 (9)
O(9)	5630 (15)	124 (9)	6353 (13)	83 (10)
O(10)	6955 (24)	398 (24)	7489 (19)	145 (22)
Cl(2A)	6372 (35)	−31 (28)	7391 (26)	57 (16)
O(7A)	5345 (53)	−113 (33)	7611 (30)	74 (22)
O(8A)	6359 (32)	657 (21)	7236 (21)	36 (13)
O(9A)	6941 (24)	−154 (14)	8146 (17)	43 (12)
O(10A)	6728 (38)	−410 (24)	6924 (24)	84 (15)
Cl(3)	3936 (3)	1770 (2)	7777 (2)	37 (2)
O(11)	3306 (9)	1257 (5)	7265 (5)	53 (5)
O(12)	4882 (9)	1992 (6)	7558 (6)	60 (5)
O(13)	4320 (10)	1462 (7)	8501 (6)	89 (6)
O(14)	3283 (12)	2371 (7)	7803 (10)	121 (9)
Cl(4)	9780 (3)	946 (2)	3764 (2)	34 (2)
O(15)	8856 (8)	1446 (5)	3581 (5)	39 (4)
O(16)	10792 (8)	1339 (6)	4015 (6)	62 (5)
O(17)	9750 (9)	555 (5)	3109 (5)	50 (5)
O(18)	9678 (11)	471 (6)	4337 (6)	84 (6)
O(1W)	7448 (8)	2712 (5)	3625 (5)	49 (5)
O(2W)	6563 (14)	4088 (9)	3937 (8)	64 (8)
O(3W)	4232 (27)	9554 (16)	849 (16)	39 (13)

[a] Equivalent isotropic *U* defined as one-third of the trace of the orthogonalized $\mathbf{U}_{ij}$ tensor.

Table III. Cyclic Voltammetric Data for Bis(μ-oxo)dimanganese(III,IV) Complexes[a]

complex	ligand	(III,III) ↔ (III,IV)	(III,IV) ↔ (IV,IV)
	bispicen[b]	0.125	0.959
8	bispictn	0.132	1.008
9	bispicpn	0.170	0.976
10	bispicbn	0.120	0.957
11	bispichxn	0.148	0.968
12	Me_2bispicen	0.083	0.943
13	Me_2bispictn	0.160	0.986

[a] Solutions were 2 mM in acetonitrile with 0.1 M Et_4NClO_4 as supporting electrolyte. Values are reported vs Ag/AgCl. Scan speed: 100 mV/s. [b] Values from ref 7.

Table IV. Absorption Spectra for Bis(μ-oxo)dimanganese Complexes

complex	ligand λ, nm (ϵ, $M^{-1}\ cm^{-1}$)
	$Mn^{III}Mn^{IV}$ Complexes
	bispicen 659 (500), 553 (535), 444 (sh 1077), 385 (sh 1277)
8	bispictn 664 (461), 554 (396), 440 (sh 1001), 385 (sh 1311)
9	bispicpn 658 (451), 551 (485), 440 (sh 1085), 385 (sh 1385)
10	bispicbn 658 (456), 551 (516), 440 (sh 1117), 385 (sh 1403)
11	bispichxn 658 (496), 551 (562), 440 (sh 1242), 385 (sh 1720)
12	Me_2bispicen 661 (400), 555 (404), 445 (sh 892), 390 (sh 1099)
13	Me_2bispictn 671 (482), 555 (382), 448 (sh 917), 390 (sh 1362)
	Mn^{IV}_2 Complexes
	bispicen 801 (80), 631 (638), 543 (857), 470 (sh 1544), 411 (3956)
14	bispictn 800 (87), 630 (516), 543 (581), 470 (sh 1127), 401 (2994)
15	bispicbn 800 (79), 630 (644), 540 (902), 470 (sh 1758), 409 (4657)
16	bispichxn 800 (80), 630 (625), 545 (919), 470 (sh 1945), 409 (5350)

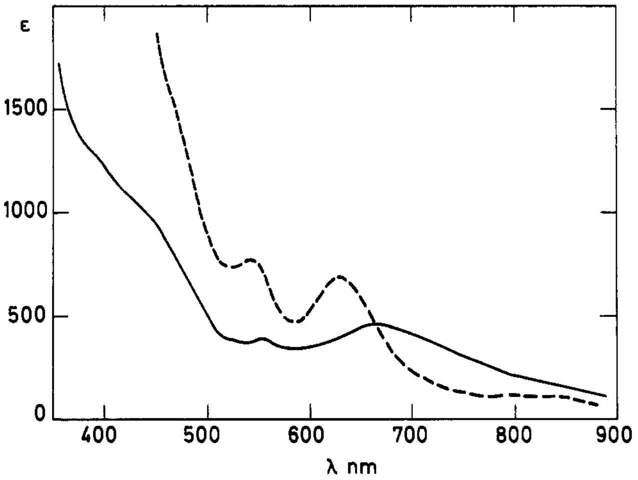

Figure 1. Electronic absorption spectra of the (III,IV) and (IV,IV) bispictn complexes **8** and **14** in acetonitrile. The spectrum of the (III,IV) complex **8** is shown as the solid line, while that of the (IV,IV) complex **14** is shown as the dashed line.

Mn^{III}_2 species as the stabilized form.[6,10]

Spectroscopy. The electronic spectra of the $Mn^{III}Mn^{IV}$ derivatives are compared in Table IV. For each complex, the spectra consist of two intense maxima in the UV region and two bands of medium intensity in the visible region. A representative spectrum, that of the bispictn complex **8**, is displayed in Figure 1.

For the chiral ligands bispic-$(-)_D$-pn (**9**) and bispic-$(-)_D$-chxn (**11**) we are only able to isolate the $(+)_D$ isomers. The CD spectra (visible region) of $(+)_D$-[(bispic-$(-)_D$-pn)MnO_2Mn(bispic-$(-)_D$-pn)]$(ClO_4)_3 \cdot 5H_2O$ and $(+)_D$-[(bispic-$(-)_D$-chxn)MnO_2Mn-

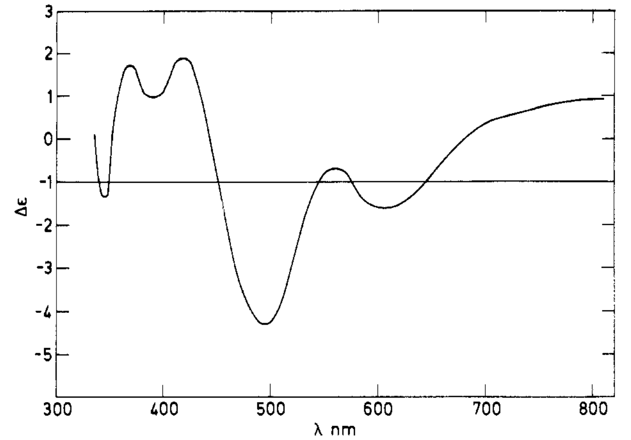

Figure 2. Circular dichroism spectrum of the (III,IV) bispichxn complex **11** in water.

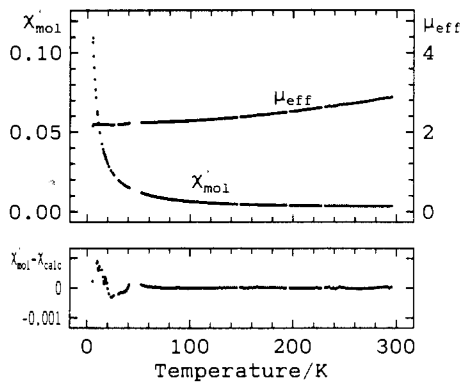

Figure 3. Magnetic susceptibility (left scale) and effective magnetic moment (right scale) of the (III,IV) complex **8**.

(bispic-$(-)_D$-chxn)]$(ClO_4)_3{\cdot}5H_2O$ are entirely similar and represent the first published CD spectra of mixed-valence $Mn^{III}Mn^{IV}$ complexes to our knowledge. They may be of value for purposes of identification, and that of the bispic-$(-)_D$-chxn complex (**11**) is shown in Figure 2. Unfortunately, we have so far been unable to grow suitable crystals of any optically active complex, so it has not yet been possible to establish any correlation between structure and the CD spectral properties as was the case in analogous chromium(III) chemistry.[26]

Magnetic Susceptibility. The temperature dependence of the magnetic susceptibility of powdered samples of the mixed-valent (III,IV) complexes **8–13** were measured in the range 4–296 K. As is shown in Figure 3, for complex **8**, the effective magnetic moment at room temperature is approximately 2.90 μ_B, declining monotonically to a value of 2.1 μ_B at 20 K; the moment is essentially constant below 20 K. The value of 2.1 μ_B corresponds fairly well to the value of $3^{1/2}\mu_B$ expected for the spin-only moment of a complex with one unpaired electron and indicates that the ground state is a doublet.

The temperature dependence of the magnetic susceptibility $\chi'_{\text{mol,exp}}$ was approximated by

$$\chi'_{\text{mol,exp}} \approx \chi'_{\text{mol,calc}} = -\frac{N}{H}\,\frac{\sum_i \frac{\partial E_i}{\partial H}\exp(-E_i/kT)}{\sum_i \exp(-E_i/kT)} + K + C/T$$

by minimization of

$$\sum_T \frac{[\chi'_{\text{mol,exp}}(T) - \chi'_{\text{mol,calc}}(T)]^2}{\sigma^2(\chi') + \left(\dfrac{\partial\chi}{\partial T}\right)^2 \sigma^2(T)}$$

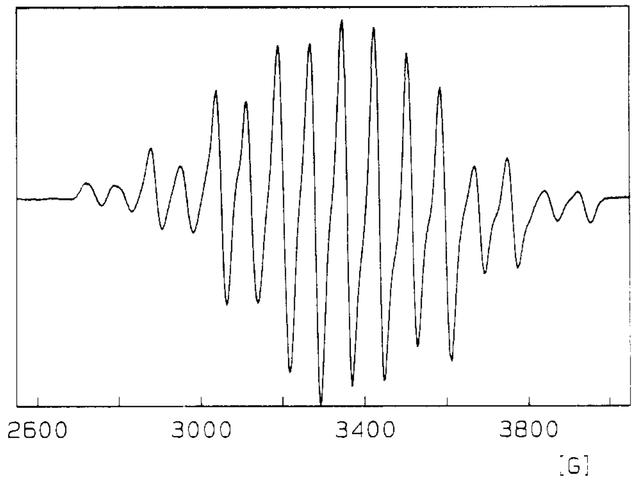

Figure 4. EPR spectrum (4.1 K) of the (III,IV) complex **12**. The spectra of complexes **9–11** are substantially similar to this, while those of **8** and **13** show more anisotropy.

within the framework of nonlinear regression analysis. The quantities $\sigma(\chi')$ and $\sigma(T)$ are the estimated standard deviations on the measured values of the magnetic susceptibility and temperature, respectively. The term C/T accounts for paramagnetic impurities, and K accounts for TIP (temperature independent paramagnetism) and minor deviations in the correction for the diamagnetic contribution of the atoms. The energies E_i of the 20 components of the ground-state manifold were obtained using the spin Hamiltonian operator

$$H = -2J\vec{S}_1{\cdot}\vec{S}_2 + g_1\beta\vec{S}_1{\cdot}\vec{H} + g_2\beta\vec{S}_2{\cdot}\vec{H}$$

where we have assumed that the g values for the two manganese atoms are identical, i.e. we have set $g_1 = g_2$. The Heisenberg term $-2J\vec{S}_1{\cdot}\vec{S}_2$ gives energies of the quartet, sextet, and octet states of $-3J$, $-8J$, and $-15J$, respectively, relative to the doublet ground state. For complex **8**, the fitting leads to a value of $2J = -405 \pm 10$ cm^{-1}. For the six complexes studied here, the values of J range from -144 ± 1 (complex **13**) to -272 ± 7 cm^{-1} (complex **12**). These values can be compared to those of -118 to -221 cm^{-1} observed for other mixed-valent bis(μ-oxo)dimanganese(III,IV) complexes.[3b,7–9,11,13,27] In the absence of detailed structural data for all of these complexes, we cannot ascribe this observed variation in the magnitude of J to any specific structural effect, but it is noteworthy that in related binuclear systems there is a correlation between the magnitude of J and the geometry of the bridging $(MO)_2$ unit.[28,29]

EPR Spectra. The EPR spectra of the (III,IV) complexes **8–13** were measured at 4.1 K; the spectrum of **12**, which exhibits the least anisotropy, is presented in Figure 4 and shows the familiar 16-line pattern.[7,9,27] The experimental spectrum was simulated by generating the energy matrix for the doublet state ($S = {}^1/_2$) for each orientation of the magnetic field relative to the molecular z axis. The energy matrix was calculated by means of the Hamiltonian operator (1), where the two hyperfine terms have been included and where $S_1 = 2$, $S_2 = {}^3/_2$.

$$A_1\vec{S}_1{\cdot}\vec{I}_1 + A_2\vec{S}_2{\cdot}\vec{I}_2 \qquad (1)$$

The resonance condition for each transition was found by successive diagonalizations and iterations, and the relative intensity was calculated from the eigenvectors. Summation of all the transitions over all space gives the simulated spectrum. The simulation programs have been used elsewhere in another con-

---

(26) Mason, S. F. *Q. Rev., Chem. Soc.* **1963**, *17*, 20–66.

(27) Cooper, S. R.; Dismukes, G. C.; Klein, M. P.; Calvin, M. *J. Amer. Chem. Soc.* **1978**, *100*, 7248–7252.

(28) Crawford, V. H.; Richardson, H. W.; Wasson, J. R.; Hodgson, D. J.; Hatfield, W. E. *Inorg. Chem.* **1976**, *15*, 2107–2110.

(29) Glerup, J.; Hodgson, D. J.; Pedersen, E. *Acta Chem. Scand., Ser. A* **1983**, *A37*, 161–164.

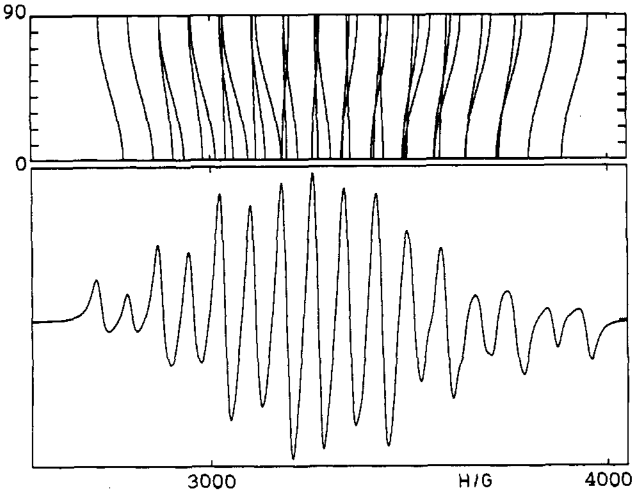

Figure 5. Simulated EPR spectrum of complex **12**, calculated using the parameters $A_{1x} = A_{1y} = -0.0078$ cm^{-1}, $A_{1z} = -0.0066$ cm^{-1}, $A_{2x} = A_{2y} = A_{2z} = -0.0074$ cm^{-1}, and $g_1 = g_2 = 2.00$. The upper graph shows the angular dependence of the resonance condition, where the ordinate is the angle between the magnetic field and the molecular *z* axis.

Table V. Selected Bond Lengths (Å)

Mn(1)–Mn(2)	2.719 (3)	Mn(1)–O(1)	1.789 (8)
Mn(1)–O(2)	1.823 (8)	Mn(1)–N(1A)	1.993 (10)
Mn(1)–N(2A)	2.042 (10)	Mn(1)–N(1B)	1.999 (10)
Mn(1)–N(2B)	2.070 (10)	Mn(2)–O(1)	1.802 (8)
Mn(2)–O(2)	1.799 (8)	Mn(2)–N(1C)	1.995 (10)
Mn(2)–N(2C)	2.056 (10)	Mn(2)–N(1D)	2.021 (10)
Mn(2)–N(2D)	2.053 (11)		

text.[30,31] Simulation by diagonalization of the energy matrix instead of by the usual perturbation treatment[27] has the advantage of giving more reliable results but it is more time consuming. The simulated spectrum in Figure 5 is calculated with the following parameter values: $A_{1x} = A_{1y} = -0.0078$ cm^{-1}, $A_{1z} = -0.0066$ cm^{-1}, $A_{2x} = A_{2y} = A_{2z} = -0.0074$ cm^{-1}, and $g_1 = g_2 = 2.00$. Figure 5 also gives the resonance condition for the 36 allowed transitions as a function of the angle between the molecular *z* axis and the magnetic field.

The spectra of **8** and **13** show the significant anisotropy seen in the phen, bpy, and tmpa derivative spectra,[9,27] but (as is the case in the bispicen complex[7]) the spectra of the other four complexes do not.

The Mn$^{IV}_2$ Complexes. Description of the Structure of 14. The structure of the (IV,IV) complex **14** consists of [(bispictn)MnO]$_2^{4+}$ cations, perchlorate anions, and water molecules. A view of the cation is given in Figure 6. Principal bond distances and angles are listed in Tables V and VI, respectively.

The geometry about each manganese center is roughly octahedral, the ligating atoms being two cis oxo bridges and the four nitrogen atoms from the pyridyl and amino groups in the bispictn ligand. As was the case for the bispicen (IV,IV) and (III,IV) dimers,[4,7] the isomer isolated here is the α,α form in which the pyridine nitrogen atoms are trans at both metal centers. This is only one of the isomers possible with this ligand; the β,β form in which the pyridine groups are cis at both metal centers was found in the complex ion [(bispictn)Cr(OH)]$_2^{4+}$,[20] and the α,β form in which the pyridine groups are trans at one metal center and cis at the other was found in a chromium dimer containing the bispicen ligand.[19]

The Mn–Mn separation of 2.719 (3) Å falls within the range of 2.625 (2)–2.748 (2) Å observed for other structurally characterized bis(μ-oxo)dimanganese(IV,IV) complexes,[3b,7,9,16,17] and is only slightly longer than the value of 2.672 (1) Å found in the analogous bispicen (IV,IV) complex.[7] The Mn–O–Mn angles of 97.3 (4) and 98.4 (4)° are slightly larger than the corresponding angles 95.2 and 95.0° in the bispicen (IV,IV) complex, which is consistent with the longer Mn–Mn separation in **14**, and fall in the range of 91.9 (2) to 101.5 (15)° observed for other bis(μ-oxo)dimanganese(IV,IV) complexes.[3b,7,9,16,17] The trans N–Mn–N angles defined by the axial pyridine groups are 165.9 (4) and 166.5 (4)°, again similar to the values of 166.7 (1) and 171.6 (1)° in the bispicen (IV,IV) complex.

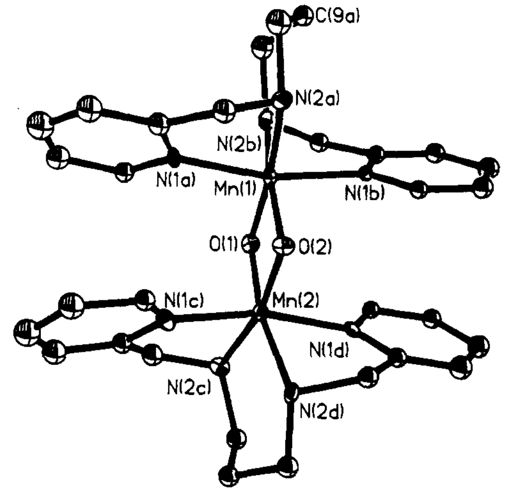

Figure 6. View of the cation in the Mn$^{IV}_2$ complex **14**. The atom labeled C(9a) is the disordered carbon atom; the position shown in the figure is that of the 75.5% contributor (see text).

Table VI. Selected Bond Angles (deg)

O(1)–Mn(1)–O(2)	82.0 (4)	O(1)–Mn(1)–N(1A)	94.3 (4)
O(2)–Mn(1)–N(1A)	96.7 (4)	O(1)–Mn(1)–N(2A)	170.4 (4)
O(2)–Mn(1)–N(2A)	92.1 (4)	N(1A)–Mn(1)–N(2A)	78.8 (5)
O(1)–Mn(1)–N(1B)	97.3 (4)	O(2)–Mn(1)–N(1B)	91.8 (4)
N(1A)–Mn(1)–N(1B)	166.5 (4)	N(2A)–Mn(1)–N(1B)	90.4 (4)
O(1)–Mn(1)–N(2B)	87.6 (4)	O(2)–Mn(1)–N(2B)	166.1 (4)
N(1A)–Mn(1)–N(2B)	93.3 (4)	N(2A)–Mn(1)–N(2B)	99.3 (4)
N(1B)–Mn(1)–N(2B)	80.3 (4)	O(1)–Mn(2)–O(2)	82.3 (4)
O(1)–Mn(2)–N(1C)	100.0 (4)	O(2)–Mn(2)–N(1C)	91.8 (4)
O(1)–Mn(2)–N(2C)	86.8 (4)	O(2)–Mn(2)–N(2C)	165.8 (5)
N(1C)–Mn(2)–N(2C)	81.2 (4)	O(1)–Mn(2)–N(1D)	92.9 (4)
O(2)–Mn(2)–N(1D)	95.6 (4)	N(1C)–Mn(2)–N(1D)	165.9 (4)
N(2C)–Mn(2)–N(1D)	94.0 (4)	O(1)–Mn(2)–N(2D)	169.9 (4)
O(2)–Mn(2)–N(2D)	94.1 (4)	N(1C)–Mn(2)–N(2D)	89.5 (4)
N(2C)–Mn(2)–N(2D)	98.1 (4)	N(1D)–Mn(2)–N(2D)	77.9 (4)
Mn(1)–O(1)–Mn(2)	98.4 (4)	Mn(1)–O(2)–Mn(2)	97.3 (4)

The average axial Mn–N bond length of 2.002 (13) Å is shorter than the average equatorial bond length of 2.055 (12) Å. This difference can be attributed to the trans influence of the bridging oxo groups, since in the phen (IV,IV) complex the average axial Mn–N bond is 0.067 Å longer than the average equatorial bond.[3b] These distances are similar to the average values of 2.007 (3) and 2.060 (3) Å found for the axial and equatorial Mn–N bonds, respectively, in the bispicen (IV,IV) complex.[7] This similarity between the axial and equatorial distances is as expected for a spherically symmetric d^3 manganese(IV) ion. The average Mn–O distance of 1.803 (14) Å compares well with the range of values 1.750 (31)–1.819 (3) Å reported for the other (IV,IV) complexes.

The geometry of the bispictn ligands is unremarkable except for disorder of the ligand on Mn(1) about the central carbon of the propane bridge. The structure refines to a ratio of 75.5:24.5 for the relative amounts of the disordered methylene group between the two conformations.

Spectroscopy. The electronic spectra of the Mn$^{IV}_2$ derivatives are compared to those for the (III,IV) complexes in Table IV. For each (IV,IV) complex, the spectra again consist of two intense maxima in the UV region and two bands of medium intensity in the visible region. A representative spectrum, that of the bispictn complex **14**, is compared with that of the (III,IV) analogue in Figure 1. The CD spectrum (visible region) of (+)$_D$-[(bispic-(–)$_D$-chxn)MnO$_2$Mn(bispic-(–)$_D$-chxn)](ClO$_4$)$_4$·4H$_2$O (**16**) is shown in Figure 7. The spectrum is the first CD spectrum of

---

(30) Bang, E.; Eriksen, J.; Glerup, J.; Mønstad, L.; Mønstad, O.; Weihe, H. *Acta Chem. Scand.* **1991**, *45*, 367–372.

(31) Glerup, J.; Weihe, H. *Acta Chem. Scand.* **1991**, *45*, 444–448.

Table VII. Parameters Derived from the Magnetic Susceptibility Data for Mn^{IV}_2 Complexes

L	model[a]	$-2J$, cm^{-1}	j, cm^{-1}	$E(1)$, cm^{-1}	$E(2)$, cm^{-1}	$E(3)$, cm^{-1}	g	var/f[b]
bispicen	1	253 (1)		253	759	1518	1.95	14
	2	296 (6)	−6 (1)	260	812	1726	2.00	9.2
bispictn	1	211 (1)		211	633	1266	1.83	15
	2	296 (3)	−11 (1)	225	740	1677	1.95	3.1
bispic-(−)-pn	1	248 (1)		248	744	1487	1.96	21
	2	271 (8)	−3 (1)	249	768	1597	1.99	13
bispicbn	1	243 (2)		243	729	1458	1.84	53
	2	403 (13)	−22 (2)	260	912	2220	2.00	18
bispic-(−)-chxn	1	232 (1)		232	696	1392	1.85	68
	2	353 (11)	−17 (2)	243	830	1965	2.00	25
Me_2bispicen	1	237 (1)		237	711	1422	1.88	10
	2	291 (4)	−7 (1)	244	775	1680	1.96	4.2

[a] Model 2 includes a biquadratic term; see text. [b] The variance/degree of freedom, a measure of the quality of the fit.

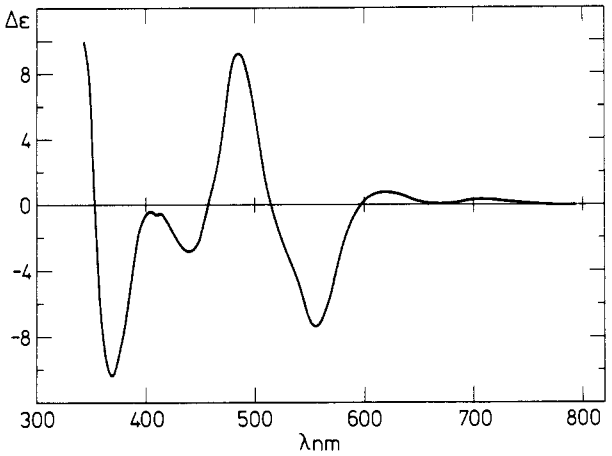

Figure 7. Circular dichroism spectrum of the (IV,IV) bispichxn complex **16** in acetonitrile.

this type of complex to be published to our knowledge and may be of value for purposes of identification. In the region of the d–d transitions the spectrum is reminiscent of that of the $(+)_D$-$[(bispic\text{-}(-)_D\text{-}pn)Cr(OH)_2Cr(bispic\text{-}(-)_D\text{-}pn)]^{4+}$ ion, to which we have earlier assigned the ΛΛ-configuration at the metal centers.[32]

Magnetic Susceptibility. The temperature dependence of the magnetic susceptibility of powdered samples of the (IV,IV) complexes **14**, **15**, and **16** were measured in the range 4–296 K. As is shown in Figure 8, for complex **14**, the effective magnetic moment at room temperature is approximately 2.50 μ_B, declining monotonically to a value of 1.0 μ_B at 45 K; the moment is essentially constant below 45 K. Presumably, the observed moment below 45 K is the result of the presence of a small quantity of the (III,IV) complex or of some monomeric material. Similar magnetic properties were observed for other (IV,IV) complexes. The susceptibility data were fitted as above, but since we have two $S = {}^3/_2$ centers in the (IV,IV) complexes the Heisenberg term in the Hamiltonian gives rise to a singlet, a triplet, a quintet, and a septet state, with energies of 0, $-2J$, $-6J$, and $-12J$, respectively.

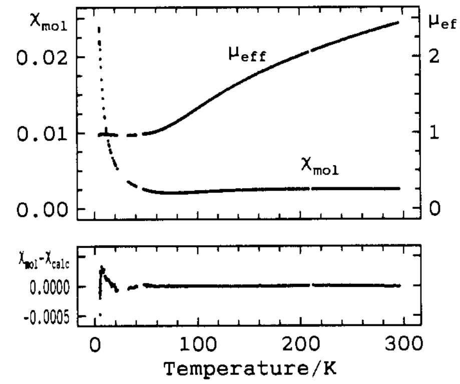

Figure 8. Magnetic susceptibility (left scale) and effective magnetic moment (right scale) of the (IV,IV) complex **14**.

The fits of the magnetic susceptibility data of the Mn^{IV}_2 complexes are listed in Table VII. Two models were used: model 1 uses the simple Heisenberg Hamiltonian above while model 2 includes a biquadratic term of the type $-j(S_a{\cdot}S_b)^2$. For comparison, the energies of the individual spin states $E(S)$ relative to the ground-state singlet energy $E(0)$ have been calculated for both models. The quality of the fitting is relatively low for all complexes studied because of the presence, in all cases, of small but magnetically significant amounts of Mn(II) impurities. The fitting leads to a value of the singlet–triplet separation $E(1)$ in the range 225–260 cm^{-1} using the data obtained from model 2. These values can be compared to those of 251.2, 262, 274, and 288 cm^{-1} for the bispicen,[7] tmpa derivative,[9] tmpa,[15] and phen[3b] complexes, respectively. There is no obvious correlation between J and the bridging geometry in this series of structurally and magnetically characterized (IV,IV) complexes.

Acknowledgment. This work was supported by the National Science Foundation through Grant No. CHE-9007607 (to D.J.H.) and by the Scientific Affairs Division, North Atlantic Treaty Organization (NATO), through Grant No. CRG 910277 (to D.J.H. K.M., and J.G.).

Supplementary Material Available: Tables S1 (hydrogen atom parameters for **14**), S2 (anisotropic thermal parameters for **14**), S3 (bond lengths for **14**), and S4 (bond angles for **14**) (4 pages); a tabulation of observed and calculated structure amplitudes for **14** (17 pages). Ordering information is given on any current masthead page.

---

(32) Michelsen, K.; Pedersen, E. *Acta Chem. Scand., Ser. A* **1983**, *A37*, 141–152.